

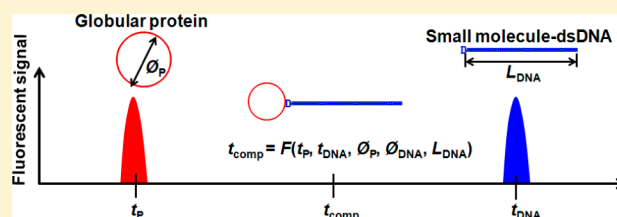
# Prediction of Protein–DNA Complex Mobility in Gel-Free Capillary Electrophoresis

Jiayin Bao,<sup>†</sup> Svetlana M. Krylova,<sup>†</sup> Leonid T. Cherney,<sup>†</sup> Robert L. Hale,<sup>‡</sup> Svetlana L. Belyanskaya,<sup>‡</sup> Cynthia H. Chiu,<sup>‡</sup> Christopher C. Arico-Muendel,<sup>‡</sup> and Sergey N. Krylov<sup>\*,†</sup>

<sup>†</sup>Department of Chemistry and Centre for Research on Biomolecular Interactions, York University, Toronto, Ontario M3J 1P3, Canada

<sup>‡</sup>GlaxoSmithKline, 343 Winter Street, Waltham, Mississippi 02451-8714, United States

**ABSTRACT:** Selection of protein binders from highly diverse combinatorial libraries of DNA-encoded small molecules is a highly promising approach for discovery of small-molecule drug leads. Methods of kinetic capillary electrophoresis provide the high efficiency of partitioning required for such selection but require the knowledge of electrophoretic mobility of the protein–ligand complex. Here we present a theoretical approach for an accurate estimate of the electrophoretic mobility of such complexes. The model is based on a theory of the thin double layer and corresponding expressions used for the mobilities of a rod-like short oligonucleotide and a sphere-like globular protein. The model uses empirical values of mobilities of free protein, free ligand, and electroosmotic flow. The model was tested with a streptavidin–dsDNA complex linked through biotin (small molecule). The deviation of the prediction from the experimental mobility did not exceed 4%, thus confirming that not only is the model adequate but it is also accurate. This model will facilitate reliable use of KCE methods for selection of drug leads from libraries of DNA-encoded small molecules.



Selection of protein binders from highly diverse combinatorial libraries (complex mixtures) of molecules is an efficient and economical alternative to traditional screening for discovery of affinity probes and drug leads.<sup>1</sup> The molecules in the most diverse libraries, with only ~1–100 copies of every molecule present in a sample, include either DNA or RNA for the purpose of binder identification. The unique property of DNA is that it can be amplified by PCR and sequenced to reveal the binder's identity. RNA, on the other hand, can be easily converted into DNA, which can then be amplified and sequenced. The examples of such libraries are (i) random DNA (or RNA) libraries used for selection of oligonucleotide aptamers,<sup>2,3</sup> (ii) mRNA-display libraries containing chimeras of mRNAs with peptides that they encode and used to select protein-binding peptides,<sup>4</sup> and (iii) DNA-encoded libraries of small molecules used for selection of small-molecule protein binders.<sup>5</sup> For any specific library, the oligonucleotides have identical lengths and are the bulkiest parts of the molecules. They largely define the physical properties of the library molecules such as size and electrical charge, so that other parts, even when present, can be neglected if these physical properties are of major importance. Therefore, for a general consideration considering only the physical properties of molecules, we can assume that the protein binds DNA and we will use this simplification unless the details are essential.

In the binder selection procedure, the library is mixed with the protein target to allow library molecules to bind the target. The target-bound molecules are partitioned from the target-unbound ones. The collected bound molecules are dissociated

from the protein and identified by sequencing their DNA (or DNA complement of RNA). The partitioning step must be very efficient to ensure that the binders are not lost while the non-binders are removed. Typically, partitioning is done by using surface-based approaches: separation on filters that retain the protein but let DNA (RNA) through or affinity chromatography with the protein immobilized on the stationary phase and retaining the binders.<sup>6</sup>

Surface-based techniques suffer from low partitioning efficiency caused by nonspecific binding of the library molecules to the surface of the filter or the stationary phase. The fraction of the library that nonspecifically binds to the surface can be as high as 15%.<sup>7</sup> Such a high background decreases the efficiency of the selection procedure. It is especially detrimental for selection of binders from DNA-encoded libraries of small molecules. Unlike random DNA libraries and mRNA display libraries, the libraries of DNA-encoded small molecules cannot be propagated because small molecules are not amplifiable. Therefore, enrichment of true binders must be achieved within a few rounds of selection which, in turn, requires high partitioning efficiency of separation methods used in the selection. Failure to successfully select protein binders from the three types of libraries considered here can be caused by low partitioning efficiency of the surface-based separation methods used.<sup>8</sup>

**Received:** December 3, 2014

**Accepted:** January 11, 2015

**Published:** January 11, 2015

Gel-free capillary electrophoresis (CE) is a solution-based separation technique and a highly promising alternative to surface-based techniques for partitioning protein–DNA complexes from the unbound DNA library. The separation in CE is based on different electrophoretic mobilities of DNA and protein–DNA complexes; the protein–DNA complex always has a greater friction coefficient (of the drag force) and a lower negative charge density than unbound DNA. Moreover, all DNA molecules of the same length have similar mobilities and migrate as a single electrophoretic zone. All complexes of the same-length DNA with the same protein also have similar mobilities and migrate as a single electrophoretic zone. When a bare fused silica capillary is used along with a pH-neutral separation buffer, there is always an appreciable electroosmotic flow (EOF) from the positive-electrode end to the negative-electrode end of the capillary. The absolute value of EOF mobility is greater than those of DNA and protein–DNA complexes while the direction is opposite. As a result, DNA and protein–DNA complexes injected at the positive-electrode will move toward the negative-electrode end (despite their overall negative charges) with the complexes moving faster (Figure 1A).

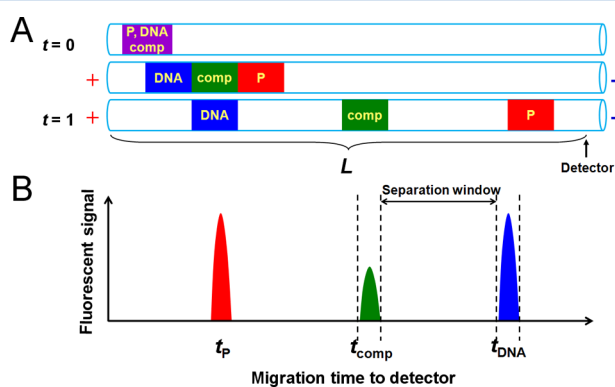


**Figure 1.** Conceptual depiction of migration patterns of DNA, protein, and complex. (A) The sample that contains DNA, protein, and complex is injected into the capillary at  $t = 0$ . Under high voltage, all three components start to migrate toward the outlet yet separate from each other based on their size to charge ratios. The complete separation is achieved at  $t = 1$ . (B) The graph illustrates the corresponding migration times of DNA, protein, and complex.

The complexes can be collected at the capillary outlet before the unbound DNA reaches the end. The greater time window between the complexes and unbound DNA will result in a greater partitioning efficiency (Figure 1B). The background can originate from unbound DNA moving along with the protein–DNA complex.<sup>9</sup> A wide time window between the zones of the complex and unbound DNA guarantees very low background which must be much lower than that of surface-based methods.<sup>10</sup>

The above advantages of gel-free CE led to its practical use for analytical and preparative separation of protein–DNA complexes. Methods of kinetic capillary electrophoresis (KCE) were successfully utilized for measuring rate constants of complex formation,  $k_{\text{on}}$ , and dissociation,  $k_{\text{off}}$ , and equilibrium dissociation constant,  $K_d$ .<sup>11–15</sup> KCE methods were also used for selection of protein binders from DNA libraries.<sup>16</sup> In particular, DNA aptamers were selected for a number of proteins.<sup>17</sup> Uniquely, KCE methods allowed selection of aptamers with desirable ranges of  $k_{\text{off}}$  and  $K_d$  values.<sup>18</sup> The library enrichment is typically completed in 1–4 rounds of partitioning in contrast

to 10–20 rounds usually required with surface based methods.<sup>19</sup> Such high speed of enrichment is explained by an extremely low level of background of <0.01%.<sup>20</sup> The use of KCE methods was also suggested for selection of protein binders from libraries of DNA-encoded small molecules, and some performance parameters have been experimentally evaluated for this application.<sup>14</sup>

Selection of protein binders from DNA libraries requires collection of a fraction of the intact protein–DNA complex (and/or free DNA that originated from the dissociation of protein–DNA complex) during electrophoresis. Accurate fraction collection requires the knowledge of migration time of protein–DNA complexes. In some instances, adding a great excess of protein to the library leads to creation of nonspecific protein–DNA complexes that can be detectable.<sup>21</sup> However, this approach does not work when the protein does not have a tendency of binding DNA nonspecifically. Blind fraction collection has high odds that either the complex will not be collected or a large amount of “background” DNA will be collected along with the complex. The latter is an indicator of inefficient partitioning that can be detrimental for selection, especially from nonamplifiable libraries of DNA-encoded small molecules. Therefore, it is of great importance for KCE-based selection of protein binders to have a method of accurate prediction of protein–DNA complex mobility. Here we present such a method for complexes of proteins with DNA-encoded small molecules. In this case we use a model of a globular protein with a rigid dsDNA attached to the protein in a single point (Figure 2). The model is based on a theory of the thin

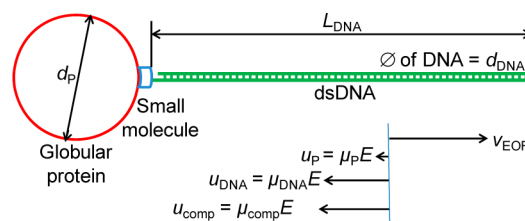


**Figure 2.** Schematic representation of the complex of globular protein and rod-like dsDNA, linked through a small molecule, capable of binding the protein. This model mimics the complex between a protein and a DNA-encoded small molecule with the dsDNA part. The lower part illustrates relative values of velocities of EOF, protein, DNA, and protein–DNA complex.

double layer and corresponding expressions used for the mobilities of a rod-like short oligonucleotide and a sphere-like globular protein. It uses empirical data for mobilities of free DNA and free protein, which can be easily determined experimentally. To test the developed mathematical model, we used binding of streptavidin to biotin-labeled dsDNA of different lengths. The results show that the model can predict the mobility of protein–DNA complex with an error of less than 4% and the travel time of protein–DNA complex to the detector with error less than 6%. It can thus aid selection of protein binders from libraries of DNA-encoded small molecules and advance the use of such libraries in identifying drug leads and diagnostic probes.

## RESULTS AND DISCUSSION

**Mathematical Model.** In this work, we concentrate on libraries of DNA-encoded small molecules in which the DNA part is dsDNA of  $\sim 120$  base pairs in length. This case describes

a class of practical libraries of DNA encoded small molecules used in the pharmaceutical selection of drug leads.<sup>22</sup>

Proteins have been used as tags to cause DNA mobility shift in DNA sequencing.<sup>23</sup> The general separation approach dealing with such molecular chimeras is termed End-Labeled Free-Resolution Electrophoresis (ELFSE) of DNA. To aid processing data from ELFSE-of-DNA experiments, theoretical models of ELFSE have been developed.<sup>24–30</sup> Such models usually employ the blob theory that is applicable to DNA which is sufficiently long to be considered a semiflexible random coil.<sup>28,30</sup> The polymer can be considered a semiflexible random coil if its contour length  $L$  is much larger than the Kuhn length  $b_K$  characterizing the polymer stiffness.<sup>31,32</sup> This assumption is not satisfied for ~120 base pairs long dsDNA for which  $L_{\text{DNA}} < 41$  nm while  $b_{K,\text{DNA}} > 100$  nm. Here and below, “DNA” in the subscript indicates that the corresponding parameter describes dsDNA. Thus, the usual ELFSE models, which are based on the blob theory, cannot be used in our case.

Taking into account that  $L_{\text{DNA}}$  is smaller than  $b_{K,\text{DNA}}$ , we use a different approach assuming that dsDNA (containing  $\leq 120$  base pairs) behaves like a rigid rod. The dsDNA diameter,  $d_{\text{DNA}}$ , can be estimated as 2 nm,<sup>33,34</sup> which is larger than the Debye length for the buffer,  $\lambda_D$ , and the dsDNA length  $L_{\text{DNA}}$  is many times larger than  $\lambda_D$ . Thus, we can assume that the dsDNA mobility,  $\mu_{\text{DNA}}$ , is estimated by an expression used in a theory of the thin double layer:<sup>24,28</sup>

$$\mu_{\text{DNA}} = \frac{\varepsilon_0 \varepsilon_r \zeta_{\text{DNA}}}{\eta} \approx \frac{-\sigma_{\text{DNA}} \lambda_D}{\eta}, \quad \left( \zeta_{\text{DNA}} \approx \frac{-\sigma_{\text{DNA}} \lambda_D}{\varepsilon_0 \varepsilon_r} \right) \quad (1)$$

Here,  $\varepsilon_0$  is the vacuum permittivity,  $\varepsilon_r$  is the relative permittivity of the buffer,  $\zeta_{\text{DNA}}$  is the zeta potential of dsDNA,  $\sigma_{\text{DNA}}$  is the surface density of the electric charge in the diffuse part of the double layer around dsDNA (i.e., excluding the Stern layer), and  $\eta$  is the dynamic viscosity of the buffer. Expression 1 can be rewritten as follows:

$$\mu_{\text{DNA}} = \frac{-\sigma_{\text{DNA}} \lambda_D}{\eta} = \frac{q_{\text{DNA}} \lambda_D}{\pi \eta d_{\text{DNA}}}, \quad \sigma_{\text{DNA}} = -\frac{q_{\text{DNA}}}{\pi d_{\text{DNA}}} \quad (2)$$

where  $q_{\text{DNA}}$  is the charge per unit length of dsDNA. In calculations of  $q_{\text{DNA}}$ , we should take into account the condensation of the counterions on dsDNA.<sup>35–39</sup> The condensation takes place for cylindrical objects with the linear density electric charge,  $q$ , satisfying relations<sup>35</sup>

$$|q| \geq q_{\text{eff}}, \quad q_{\text{eff}} = \frac{e}{z_i \lambda_B}, \quad \lambda_B = \frac{e^2}{4\pi \varepsilon_0 \varepsilon_r k_B T} \quad (3)$$

Here,  $e$  is the charge of proton,  $z_i$  is the valence of counterions,  $\lambda_B$  is the Bjerrum length,  $k_B$  is the Boltzmann constant, and  $T$  is the absolute temperature of the buffer. Usually, dsDNA has two negative charges per 0.34 nm of its length<sup>28</sup> and  $\lambda_B = 0.7$  nm for water solutions at room temperature.<sup>27,37</sup> Thus, condition 3 is always satisfied for dsDNA and condensation of counterions reduces the density of the DNA charge  $q_{\text{DNA}}$  (excluding the Stern layer) to the effective value,  $-q_{\text{eff}}$ , determined by the second relation 3.<sup>35</sup> Since we also consider the Stern layer as a part of the condensed counterion layer, then  $|q_{\text{DNA}}|$  will be even less than  $q_{\text{eff}}$ . In this case  $q_{\text{DNA}}$  can be considered as an adjustable parameter. We should note that the dsDNA mobility has negative values since dsDNA is negatively charged. Expression 2 for  $\mu_{\text{DNA}}$  can be also obtained from the balance

of electric and hydrodynamic forces,  $F_{E,\text{DNA}}$  and  $F_{H,\text{DNA}}$ , acting upon dsDNA:

$$F_{E,\text{DNA}} + F_{H,\text{DNA}} = 0 \quad (4)$$

if we assume the following effective values for these forces:

$$F_{E,\text{DNA}} = q_{\text{DNA}} L_{\text{DNA}} E, \quad F_{H,\text{DNA}} = -\frac{\pi \eta d_{\text{DNA}} L_{\text{DNA}}}{\lambda_D} u_{\text{DNA}} \quad (5)$$

Here,  $E$  is the electric field strength and  $u_{\text{DNA}}$  is a relative velocity of dsDNA with respect to the buffer. Hereafter we use a coordinate system in which electric and hydrodynamic forces have only  $x$ -components.

The average diameter  $d_p$  of a globular protein with the molecular weight  $> 10$  kDa can be estimated as 3 nm.<sup>40</sup> Thus,  $d_p$  is significantly larger than  $\lambda_D$ . In this case, the protein mobility  $\mu_p$  can be determined by expression similar to expression 1:

$$\mu_p = \frac{\varepsilon_0 \varepsilon_r \zeta_p}{\eta} \approx \frac{-\sigma_p \lambda_D}{\eta}, \quad \left( \zeta_p \approx \frac{-\sigma_p \lambda_D}{\varepsilon_0 \varepsilon_r} \right) \quad (6)$$

Here,  $\zeta_p$  is the zeta potential of the globular protein, and  $\sigma_p$  is the average surface density of the electric charge in the diffuse part of the double layer around the protein (i.e., excluding the Stern layer). Expression 6 can be also rewritten as follows:

$$\mu_p = \frac{-\sigma_p \lambda_D}{\eta} = \frac{Q_p \lambda_D}{\pi \eta d_p^2}, \quad \sigma_p = -\frac{Q_p}{\pi d_p^2} \quad (7)$$

where  $Q_p$  is the electric charge of protein (including the Stern layer charge). We should note that the protein mobility can have both positive and negative values (for positively and negatively charged proteins, respectively).

Expression 7 for  $\mu_p$  can also be obtained from the balance of electric and hydrodynamic forces,  $F_{E,p}$  and  $F_{H,p}$ , acting upon the protein molecule:

$$F_{E,p} + F_{H,p} = 0 \quad (8)$$

if we assume the following effective values for these forces:

$$F_{E,p} = Q_p E, \quad F_{H,p} = -\frac{\pi \eta d_p^2}{\lambda_D} u_p \quad (9)$$

Here,  $u_p$  is the relative velocity of the protein with respect to the buffer.

The mobility of dsDNA with a globular protein attached to its end can be found from the balance of all effective forces acting upon such a complex:

$$F_{E,\text{DNA}} + F_{E,p} + F_{H,\text{DNA}} + F_{H,p} = 0 \quad (10)$$

Substitution of expressions 5 and 9 into eq 10 gives

$$(q_{\text{DNA}} L_{\text{DNA}} + Q_p) E = \left( \frac{\pi \eta d_{\text{DNA}} L_{\text{DNA}}}{\lambda_D} + \frac{\pi \eta d_p^2}{\lambda_D} \right) u_{\text{comp}} \quad (11)$$

Solving this equation with respect to  $u_{\text{comp}}$  and taking into account that  $u_{\text{comp}} = \mu_{\text{comp}} E$  we obtain the complex mobility  $\mu_{\text{comp}}$ :

$$\mu_{\text{comp}} = \frac{q_{\text{DNA}} L_{\text{DNA}} + Q_p}{\frac{\pi \eta d_{\text{DNA}} L_{\text{DNA}}}{\lambda_D} + \frac{\pi \eta d_p^2}{\lambda_D}} \quad (12)$$

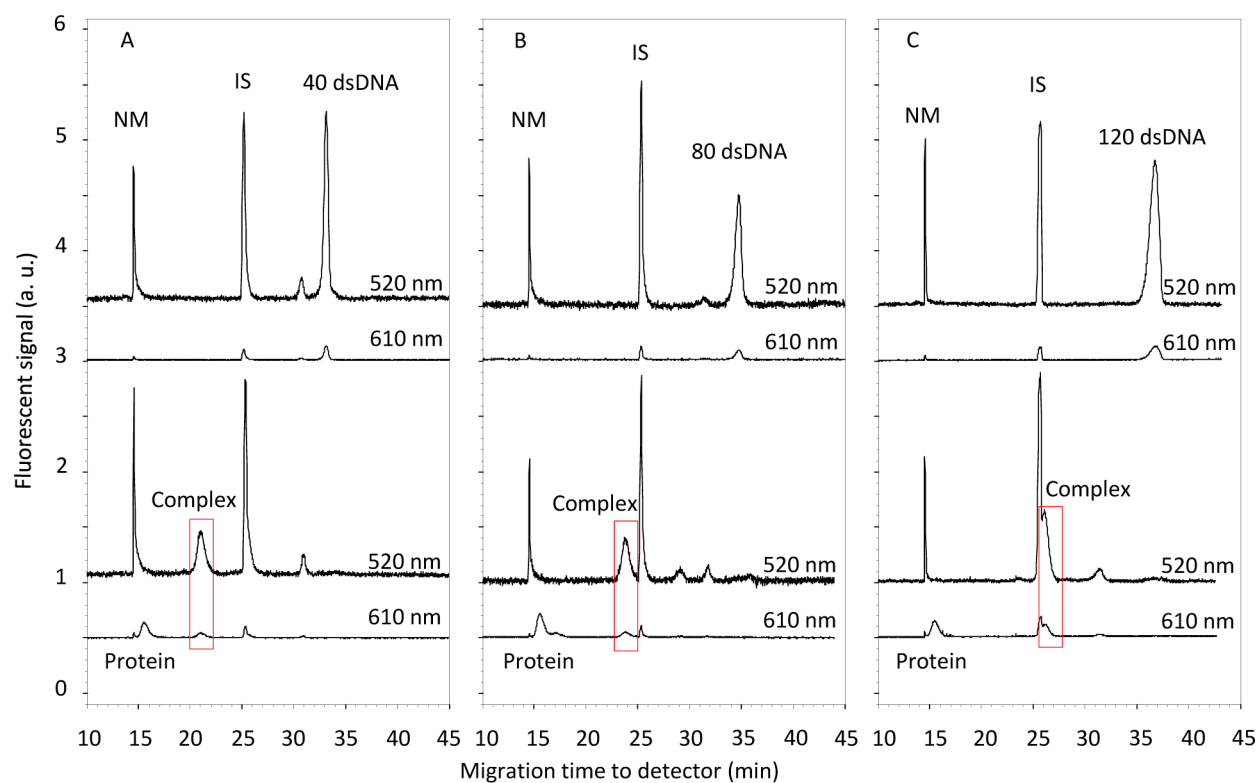


**Figure 3.** Migration information on all components. The migration patterns of 40, 80, and 120 dsDNA are shown in parts A, B, and C, respectively. In each panel, the top two traces represent a control experiment with different detection wavelengths. The control contains 100 nM dsDNA, the neutral marker (NM), and the internal standard (IS). The bottom two traces represent binding, which has the same composition as control plus 1  $\mu$ M chroemo-streptavidin protein. The binding complex was highlighted with the red box. All experiments were performed in triplicates.

Taking into account expressions 2 and 7 for the mobilities of dsDNA and the globular protein, we can rewrite the relation 12 as follows:

$$\mu_{\text{comp}} = \frac{d_{\text{DNA}}L_{\text{DNA}}\mu_{\text{DNA}} + d_{\text{p}}^2\mu_{\text{p}}}{d_{\text{DNA}}L_{\text{DNA}} + d_{\text{p}}^2} \quad (13)$$

Using expression 13 for the complex mobility, we can readily find the complex travel time to the detector,  $t_{\text{comp}}$ ,

$$t_{\text{comp}} = \frac{L}{v_{\text{EOF}} + \mu_{\text{comp}}E} \quad (14)$$

Here,  $L$  is the distance from the beginning of the capillary to the detector, and  $v_{\text{EOF}}$  is the velocity of EOF in the capillary.

It should be noted that the final expression 13 for complex mobility does not contain charges of dsDNA and protein. We excluded them using expression 2 and 6 for the mobilities of dsDNA and protein. Thus, we do not need to know the charges of dsDNA and protein to calculate complex mobility since we can experimentally determine the mobilities of dsDNA and protein. In this case, the charges of dsDNA and protein can be back calculated from relations 2 and 6 using their experimentally found mobilities and, therefore, can be considered as adjustable parameters.

**Experimental Validation of Mathematical Model.** To validate our mathematical model expressed by eqs 13 and 14, we needed a protein that binds dsDNA at its end and we needed to determine mobilities of free protein and free dsDNA as well as the EOF velocity. We chose streptavidin and biotinylated dsDNA as a binding pair. Streptavidin can bind to biotin with exceptionally high affinity. Three lengths of dsDNA

were used ( $N_{\text{DNA}} = 40, 80,$  and  $120$  base pairs) to test theory applicability for different DNA lengths. All experiments were performed in triplicates. Figure 3 shows representative electropherograms for the neutral marker (bodipy), free protein, internal standard (fluorescein), free biotinylated dsDNA, and protein–dsDNA mixture. The velocity of EOF was measured and found to be  $v_{\text{EOF}} = 0.1247 \pm 0.0002, 0.1249 \pm 0.0002,$  and  $0.1193 \pm 0.0017$  cm/s for experiments with  $N_{\text{DNA}} = 40, 80,$  and  $120$  base pairs, respectively. Mobilities of both dsDNA (in the absence of the protein) and the protein (in the absence of dsDNA) were found to be negative, which means that both dsDNA and protein are negatively charged. As a result the complex turned out to be negatively charged and its experimentally measured mobility is negative. Measurements of the dsDNA mobility resulted in the following absolute mobility values:  $|\mu_{\text{DNA}}| = 0.2678 \pm 0.0005, 0.2747 \pm 0.0014,$  and  $0.2784 \pm 0.0002$  cm<sup>2</sup>/kV s for  $N_{\text{DNA}} = 40, 80,$  and  $120$  base pairs, respectively. Measurements of the protein mobility revealed  $|\mu_{\text{p}}| = 0.0401 \pm 0.0006, 0.0403 \pm 0.0012,$  and  $0.0384 \pm 0.0006$  cm<sup>2</sup>/kV s for experiments with  $N_{\text{DNA}} = 40, 80,$  and  $120$  base pairs, respectively. Thus, the absolute value of protein mobility is significantly less than that of dsDNA. The mobilities of the complexes were found to be  $|\mu_{\text{comp}}| = 0.1643 \pm 0.0006, 0.2007 \pm 0.0022,$  and  $0.2195 \pm 0.0006$  cm<sup>2</sup>/kV s for  $N_{\text{DNA}} = 40, 80,$  and  $120$  base pairs, respectively. Thus, a complete set of experimental data required for model validation needs to be obtained.

In addition to the described experimental values of mobilities and velocities, we needed to know the hydrodynamic sizes of the streptavidin ( $d_{\text{p}}$ ) and dsDNA ( $d_{\text{DNA}}$  and  $L_{\text{DNA}}$ ). We used a value of  $d_{\text{DNA}} = 2.6$  nm, which includes the hydration shell

around dsDNA,<sup>41</sup> and a value for the streptavidin molecule diameter,  $d_p = 5.3$  nm, determined from crystallographic studies.<sup>42</sup> The dsDNA length was calculated as  $L_{\text{DNA}} = b_{\text{DNA}}N_{\text{DNA}}$ , where  $b_{\text{DNA}} = 0.34$  nm is the dsDNA monomer length.

We used the described parameters in eqs 13 and 14 to calculate predicted mobilities and travel times to the detector for protein–dsDNA complexes at different lengths of dsDNA. Figure 4 shows absolute values of the experimental and theoretical mobilities of the protein–DNA complexes. According to the results in Figure 4, the developed model

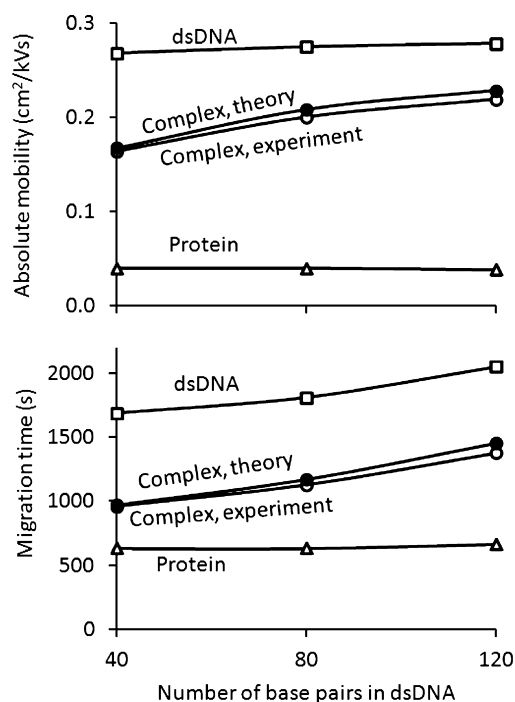


**Figure 4.** Dependences of the protein–dsDNA complex mobility (top) and travel time to the detector (bottom) on the number of base pairs in dsDNA. Mobilities and migration times of dsDNA and protein are also shown. Experimental results are shown by lines with open markers while theoretical results are shown by lines with solid markers. Theoretical values were obtained from expressions 13 and 14

can predict the mobility of the protein–DNA complex with an error of less than 4% and the travel time of the protein–DNA complex to the detector with error less than 6%. It should be noted that different models were proposed for the mobility of rigid composite objects formed by a rod and a sphere.<sup>27,43</sup> In these models, only one part (the rod or the sphere) is charged whereas in our case both parts (the rod-like dsDNA and the globular protein) can be charged. Extension of these models to our case results in the following expression for the complex mobility

$$\mu_{\text{comp}} = \frac{\xi_{\text{DNA}}\mu_{\text{DNA}} + \xi_{\text{P}}\mu_{\text{P}}}{\xi_{\text{DNA}} + \xi_{\text{P}}} \quad (15)$$

Here  $\xi_{\text{DNA}}$  and  $\xi_{\text{P}}$  are the friction coefficients of a rod and a sphere defined by relations:<sup>27,44</sup>

$$\xi_{\text{DNA}} = \frac{2\pi\eta L_{\text{DNA}}}{\ln \frac{2L_{\text{DNA}}}{d_{\text{DNA}}} - \frac{1}{2}}, \quad \xi_{\text{P}} = 3\pi\eta d_{\text{P}} \quad (16)$$

Relation 15 differs from expression 13 that we obtained and is used to predict the complex mobility. In particular, relation 15 depends on  $d_{\text{DNA}}$  only logarithmically (very weakly). Calculation based on eqs 15 and 16 give  $|\mu_{\text{comp}}| = 0.1496, 0.1748, \text{ and } 0.1909$  cm<sup>2</sup>/kV s for  $N_{\text{DNA}} = 40, 80, \text{ and } 120$  base pairs, respectively. Comparing these theoretical values of complex mobility to ones experimentally determined above we can conclude that expression 15 results in 13% relative error in prediction of complex mobility whereas our expression 13 leads to only 4% error.

To summarize, we developed an approach for accurate estimate of the mobility of the protein–dsDNA complex. The approach uses an approximation of a globular protein and a rod-like dsDNA. It will aid in selection and characterization of protein binders from libraries of DNA-encoded small molecules by methods of KCE. The general approach developed here can be utilized to develop similar models for other types of DNA libraries.

## MATERIALS AND METHODS

**Chemicals and Materials.** Fused-silica capillary was purchased from Polymicro (Phoenix, AZ). All reagents were dissolved in 50 mM Tris-HCl, pH 8.0. The 40, 80, and 120 dsDNA were synthesized by PCR, and a pETMutS plasmid was used as a template (Addgene plasmid 13245, Cambridge, MA). All DNA primers were purchased from IDT DNA Technology Inc. (Coraville, IA). DNA primer sequences were

Forward primer: FAM 5'-CCGACTACCTCCTCCTCTTC-3'  
 Reverse primer 40: Biotin 5'-TCGTAGAAGTCCCCCACCTG-3'  
 Reverse primer 80: Biotin 5'-CAGGGCGCGGGCCA-3'  
 Reverse primer 120: Biotin 5'-TGGTGAAGTCCTTGCTGGTC-3'

All PCR products were subjected onto a 2% agarose gel, and the bands that contained dsDNA were excised and purified by using a QIAquick Gel Extraction Kit (Toronto, ON, Canada). The purified dsDNA were quantified by using fluorescence detection at 520 nm. The FAM-labeled forward primer was used as a concentration standard. The streptavidin (Sigma-Aldrich, Oakville, ON, Canada) was labeled with a fluorogenic dye, Chromeo 488 (Active Motif, Carlsbad, CA) overnight at 4 °C. Bodipy was purchased from Life Technologies Inc. (Burlington, ON, Canada). All other reagents were purchased from Sigma-Aldrich (Oakville, ON, Canada). All solutions were made using deionized water filtered through a 0.22 μm filter (Millipore, Nepean, ON, Canada).

**Instrumentation.** The ABI7300 real time PCR (BioRad, Mississauga, ON, Canada) was used to synthesis dsDNA. The Owl D2 Wide-Gel Electrophoresis System (Thermo Scientific, Wilmington, DE) was used to purify the PCR products. NanoDrop 3300 fluorospectrometer (Thermo Scientific, Wilmington, DE) was used for dsDNA quantification. All CE experiments were carried out with MDQ-PACE instrument (Beckman-Coulter, ON, Canada) equipped with a laser-induced fluorescence (LIF) detector. LIF signal was recorded at 520 nm (for fluorescein, FAM, and bodipy detection) and 605 nm (for chromeo-streptavidin detection) with 4 Hz acquisition rate. The inner diameter of the capillary was 75 μm. The total capillary length was 81.2 cm with 71.2 cm from the injection end to the detection window.

**Migration Analysis by CE–LIF.** The 50 mM Tris-HCl, pH 8.0 buffer was used for both incubation and separation. The binding mixture was made by incubating 100 nM dsDNA, 1  $\mu$ M chromeo-labeled streptavidin, 10 nM fluorescein (internal standard), and 5  $\mu$ M bodipy (neutral marker), at 20 °C for 30 min. The control mixture was the same as binding mixture yet without streptavidin. The capillary was flushed prior to each CE run with 0.1 M HCl, 0.1 M NaOH, ddH<sub>2</sub>O, and buffer. The sample was injected into the capillary at 0.5 psi for 10 s. The ends of the capillary were inserted into the inlet and outlet reservoirs, and an electric field of 308 V/cm was applied to carry out electrophoresis. The temperature of the capillary was maintained at 15 °C. All experiments were performed in triplicates.

## AUTHOR INFORMATION

### Corresponding Author

\*E-mail: skrylov@yorku.ca.

### Notes

The authors declare no competing financial interest.

## ACKNOWLEDGMENTS

The work was funded by the Natural Sciences and Engineering Research Council of Canada (Grant 445390-13).

## REFERENCES

- (1) Mayr, L. M.; Bojanic, D. *Curr. Opin. Pharmacol.* **2009**, *9*, 580–588.
- (2) Oliphant, A. R.; Brandl, C. J.; Struhl, K. *Mol. Cell. Biol.* **1989**, *9*, 2944–2949.
- (3) Tuerk, C.; Gold, L. *Science* **1990**, *249*, 505–510.
- (4) Roberts, R. W.; Szostak, J. W. *Proc. Natl. Acad. Sci. U.S.A.* **1997**, *94*, 12297–12302.
- (5) Clark, M. A.; Acharya, R. A.; Arico-Muendel, C. C.; Belyanskaya, S. L.; Benjamin, D. R.; Carlson, N. R.; Centrella, P. A.; Chiu, C. H.; Creaser, S. P.; Cuozzo, J. W.; Davie, C. P.; Ding, Y.; Franklin, G. J.; Franzen, K. D.; Geffer, M. L.; Hale, S. P.; Hansen, N. J. V.; Israel, D. I.; Jiang, J.; Kavarana, M. J.; Kelley, M. S.; Kollmann, C. S.; Li, F.; Lind, K.; Mataruse, S.; Medeiros, P. F.; Messer, J. A.; Myers, P.; O’Keefe, H.; Oliff, M. C.; Rise, C. E.; Satz, A. L.; Skinner, S. R.; Svendsen, J. L.; Tang, L.; Vloten, K.; Wagner, R. W.; Yao, G.; Zhao, B.; Morgan, B. A. *Nat. Chem. Biol.* **2009**, *5*, 647–654.
- (6) Biroccio, A.; Hamm, J.; Incitti, I.; De Francesco, R.; Tomei, L. J. *Virology* **2002**, *76*, 3688–3696.
- (7) Papoulas, O. Rapid Separation of Protein-Bound DNA from Free DNA Using Nitrocellulose Filters. In *Current Protocols in Molecular Biology*; Wiley: New York, 2001; Vol. 36, 12.8.1–12.8.9.
- (8) Wang, J.; Rudzinski, J. F.; Gong, Q.; Soh, H. T.; Atzberger, P. J. *PLoS One* **2012**, *7*, e43940.
- (9) Berezovski, M.; Musheev, M.; Drabovich, A.; Krylov, S. N. *J. Am. Chem. Soc.* **2006**, *128*, 1410–1411.
- (10) Tok, J.; Lai, J.; Leung, T.; Li, S. F. Y. *Electrophoresis* **2010**, *31*, 2055–2062.
- (11) Berezovski, M.; Krylov, S. N. *J. Am. Chem. Soc.* **2002**, *124*, 13674–13675.
- (12) Bao, J.; Krylova, S. M.; Reinstein, O.; Johnson, P. E.; Krylov, S. N. *Anal. Chem.* **2011**, *83*, 8387–8390.
- (13) Bao, J.; Krylova, S. M.; Cherney, L. T.; Le Blanc, J. C. Y.; Pribil, P.; Johnson, P. E.; Wilson, D. J.; Krylov, S. N. *Anal. Chem.* **2014**, *86*, 10016–10020.
- (14) Drabovich, A. P.; Berezovski, M.; Musheev, M. U.; Krylov, S. N. *Anal. Chem.* **2009**, *81*, 490–494.
- (15) Bao, J.; Krylova, S. M.; Wilson, D. J.; Reinstein, O.; Johnson, P. E.; Krylov, S. N. *ChemBioChem* **2011**, *12*, 2551–2554.
- (16) Javaherian, S.; Musheev, M. U.; Kanoatov, M.; Berezovski, M.; Krylov, S. N. *Nucleic Acids Res.* **2009**, *37*, e62.
- (17) Hamula, C. L. A.; Guthrie, J. W.; Zhang, H.; Li, X.; Le, X. C. *Trends Anal. Chem.* **2005**, *25*, 681–691.
- (18) Drabovich, A. P.; Okhonin, V.; Berezovski, M.; Krylov, S. N. *J. Am. Chem. Soc.* **2007**, *129*, 7260–7261.
- (19) Berezovski, M.; Musheev, M. U.; Drabovich, A. P.; Jitkova, J. V.; Krylov, S. N. *Nat. Protoc.* **2006**, *1*, 1359–1369.
- (20) Musheev, M. U.; Kanoatov, M.; Krylov, S. N. *J. Am. Chem. Soc.* **2013**, *135*, 8041–8046.
- (21) Beinoravičiūtė-Kellner, R.; Lipps, G.; Krauss, G. *FEBS Lett.* **2005**, *579*, 4535–4040.
- (22) Kleiner, R. E.; Dumelin, C. E.; Liu, D. R. *Chem. Soc. Rev.* **2011**, *40*, 5707–5717.
- (23) Kim, J.; Bhinghe, A. A.; Morgan, X. C.; Iyer, V. R. *Nat. Methods* **2005**, *2*, 47–53.
- (24) Viovy, J. L. *Rev. Mod. Phys.* **2000**, *72*, 813–872.
- (25) Mayer, P.; Slater, G. W.; Drouin, G. *Anal. Chem.* **1994**, *66*, 1777–1780.
- (26) Hubert, S. J.; Slater, G. W. *Electrophoresis* **1995**, *16*, 2137–2142.
- (27) Desruisseaux, C.; Long, D.; Drouin, G.; Slater, G. W. *Macromolecules* **2001**, *34*, 44–52.
- (28) Meagher, R. J.; Won, J. I.; McCormick, L. C.; Nedelcu, S.; Bertrand, M. M.; Bertram, J. L.; Drouin, G.; Barron, A. E.; Slater, G. W. *Electrophoresis* **2005**, *26*, 331–350.
- (29) Meagher, R. J.; McCormick, L. C.; Haynes, R. D.; Won, J. I.; Lin, J. S.; Slater, A. E.; Barron, A. E. *Electrophoresis* **2006**, *27*, 1702–1712.
- (30) Long, D.; Dobrynin, A. V.; Rubinstein, M.; Ajdari, A. J. *Chem. Phys.* **1998**, *108*, 1234–1244.
- (31) Teraoka, I. *Polymer Solutions*; John Wiley & Sons: New York, 2002; p 360.
- (32) Strobl, G. R. *The Physics of Polymers: Concepts for Understanding Their Structures and Behavior*; Springer: Berlin, Germany, 2007; p 518.
- (33) Simmel, F. C.; Dittmer, W. U. *Small* **2005**, *1*, 284–299.
- (34) Krishnan, Y.; Simmel, F. C. *Angew. Chem., Int. Ed.* **2011**, *50*, 3124–3156.
- (35) Manning, G. S. *J. Chem. Phys.* **1969**, *51*, 924–933.
- (36) Manning, G. S. *J. Phys. Chem.* **1981**, *85*, 1506–1515.
- (37) Barrat, J. L.; Joanny, J. F. *Adv. Chem. Phys.* **1996**, *94*, 1–66.
- (38) Anik, N.; Airiau, M.; Labeau, M.-P.; Vuong, C.-T.; Reboul, J.; Lacroix-Desmazes, P.; Gérardin, C.; Cottet, H. *Macromolecules* **2009**, *42*, 2767–2774.
- (39) Ibrahim, A.; Koval, D.; Kašička, V.; Faye, C.; Cottet, H. *Macromolecules* **2013**, *46*, 533–540.
- (40) Protein size calculator: [www.calctool.org/CALC/prof/bio/protein\\_size](http://www.calctool.org/CALC/prof/bio/protein_size).
- (41) Schneider, B.; Patel, K.; Berman, H. M. *Biophys. J.* **1998**, *75*, 2422–2434.
- (42) Hendrickson, W. A.; Pähler, A.; Smith, J. L.; Satow, Y.; Merritt, E. A.; Phizackerley, R. P. *Proc. Natl. Acad. Sci. U.S.A.* **1989**, *86*, 2190–2194.
- (43) Long, D.; Ajdari, A. *Electrophoresis* **1996**, *17*, 1161–1166.
- (44) Happel, J.; Brenner, H. *Low Reynolds Number Hydrodynamics with Special Applications to Particulate Media*; Martinus Nijhoff Publishers: Leiden, The Netherlands, 1983; p 553.